White Light Interferometry

James C. Wyant
Optical Sciences Center, University of Arizona, Tucson, AZ 85721
jcwyant@optics.arizona.edu, http://www.optics.arizona.edu/jcwyant

ABSTRACT

White light interferometry is an extremely powerful tool for optical measurements. This paper discusses the advantages and disadvantages of white light interferometry compared to laser light interferometry. Three different white light interferometers are discussed; 1. diffraction grating interferometers, 2. vertical scanning or coherence probe interferometers, and 3. white light scatterplate interferometers.

Keywords: interferometry, metrology, optical testing, interference, optical measurements

1. INTRODUCTION

While white light interferometry is certainly not new, combining rather old white light interferometry techniques with modern electronics, computers, and software has produced extremely powerful measurement tools. Since the two individuals we are honoring at this symposium, Yuri Denisyuk and Emmett Leith, have done much in the area of white light holography and interferometry (1-7) I thought it was appropriate to make a few comments about white light interferometry. Since it would require at least one book to give a complete discussion of white light interferometry, I will be able to discuss only a few aspects.

Currently most interferometry is performed using a laser as the light source. The primary reason for this is that the long coherence length of laser light makes it easy to obtain interference fringes and interferometer path lengths no longer have to be matched as they do if a short coherence length white light source is used. The ease with which interference fringes are obtained when a white light source is used is both good and bad. It is good that it is easy to find laser light interference fringes, but it can be bad in that it can be too easy to obtain interference fringes and any stray reflections will give spurious interference fringes. Spurious interference fringes can result in incorrect measurements.

The requirement of having the paths matched to obtain interference fringes can be a real nuisance. However it can also be very good. As we will discuss in Section 3, knowing that good contrast interference fringes are obtained only when the interference paths are matched can help yield a powerful measurement tool. Furthermore, white light fringes are extremely beautiful as shown in Figure 1.

Figure 1. White light interference fringes.

For an interferometer to be a true white light achromatic interferometer two conditions need to be satisfied. First, the position of the zero order interference fringe must be independent of wavelength. Second, the spacing of the interference fringes must be independent of wavelength. That is, the position of all interference fringes, independent of order number, is independent of wavelength. Generally, in a white light interferometer only the first condition is satisfied and we do not have a truly achromatic interferometer.

In this paper we will talk about three different white light interferometers; 1. diffraction grating interferometers, 2. vertical scanning or coherence probe interferometers, and 3. white light scatterplate interferometers. While all three of these interferometers work with a white light source, only the first, the diffraction grating interferometer, is truly achromatic.

2. DIFFRACTION GRATING INTERFEROMETERS

There are many different diffraction grating interferometers. The really neat thing about grating interferometers is that they can be truly achromatic. The basic principle that makes the interference fringe spacing independent of wavelength is that the diffraction angle (or more precisely the sine of the angle) for a diffraction grating is proportional to the wavelength. For the spacing of the interference fringes to be independent of wavelength the sine of the angle between the two interfering beams must be proportional to the wavelength. Thus, gratings produce beams of light whose angles as a function of wavelength are correct to produce interference fringes whose spacing is independent of wavelength. The second requirement for a white light achromatic interferometer is that the zero order interference fringe is also independent of wavelength. Fortunately grating interferometers can be configured to satisfy both of these conditions. That is, both the fringe spacing and the position of the zero order interference fringe are independent of wavelength.

To illustrate that a grating interferometer can be achromatic we can look at a sinusoidal grating as shown in Figure 2. In this case the interferometer is illuminated with a spherical wave that is focused near the grating. Plane wave illumination would also work. A pure sinusoidal grating will give only two diffraction orders. If θ is the angle of incidence, φ is the angle of diffraction, d is the grating period and λ is the wavelength, the grating equation gives us

$$d(\mathrm{Sin}[\theta] + \mathrm{Sin}[\varphi]) = \lambda.$$

For simplicity let's assume we have small angles and the angle of incidence, θ, is zero, then

$$\phi = \frac{\lambda}{d}.$$

Thus, the angle of diffraction is proportional to the wavelength. If the light is focused a distance t from the grating, two images of the focused spot will be produced separated a distance (φ t) given by

$$focused_spot_separation = \phi t = 2\frac{\lambda}{d}t.$$

Thus, the point separation is proportional to the wavelength so the fringe spacing is independent of wavelength. The center point between the two point sources is also independent of wavelength so the position of the zero order fringe is independent of wavelength. Furthermore, the performance of the interferometer for white light extended sources is independent of wavelength since both the wavefront shear produced by this interferometer and the spatial coherence function scales with wavelength.

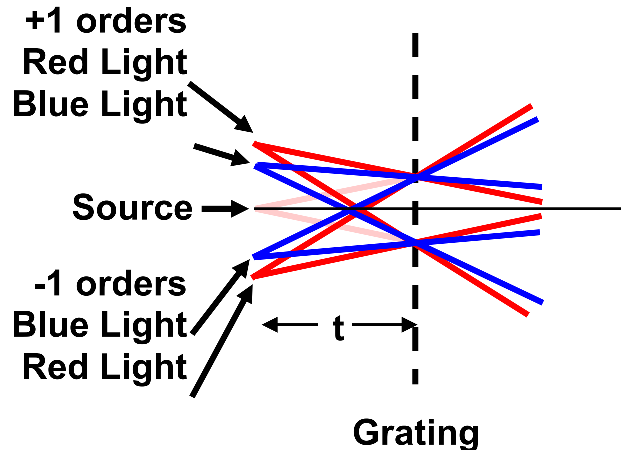

Figure 2. Sinusoidal diffraction grating illuminated with a spherical wave.

There are more complicated grating shearing interferometers than this example (8), but this simple example presents the basic idea.

3. VERTICAL SCANNING OR COHERENCE PROBE INTERFEROMETERS

Phase-shifting interferometry has proven to be extremely powerful and useful and many commercial interferometers use phase-shifting techniques. While phase-shifting interferometry has great precision, it has limited dynamic range. It can easily be shown that for phase-shifting interferometry the height difference between two adjacent data points must be less than $\lambda/4$, where λ is the wavelength of the light used. If the slope is greater than $\lambda/4$ per detector pixel then height ambiguities of multiples of half-wavelengths exist as shown in Figure 3. One technique that has been very successful in overcoming these slope limitations is to perform the measurement using two or more wavelengths. If measurements are performed using two wavelengths, λ_1 and λ_2, it can be shown that the maximum height difference between two consecutive data points is $\lambda_{eq}/4$, where λ_{eq} is given by

$$\lambda_{eq} = \frac{\lambda_1 \lambda_2}{|\lambda_1 - \lambda_2|}$$

Thus, by carefully selecting the two wavelengths it is possible to greatly increase the dynamic range of the measurement over what can be obtained using a single wavelength. (9-11).

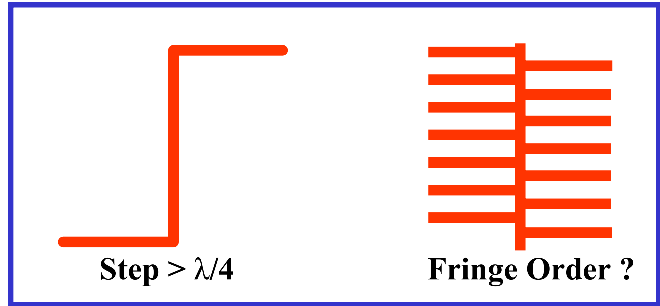

Figure 3. If a single wavelength is used and the phase step is greater than $\lambda/4$ it is difficult to connect the fringe orders on the two sides of the step.

A better approach is to use a white light source so there is no ambiguity in the fringe order number as shown in Figure 4.

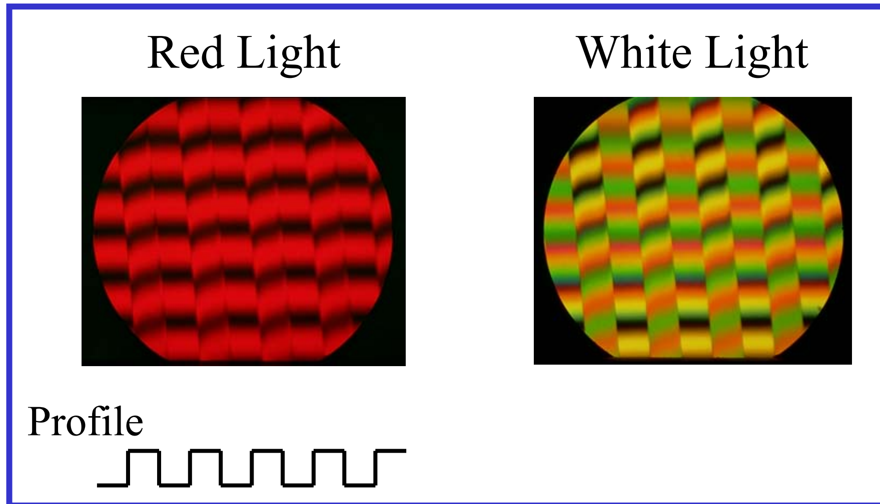

Figure 4. The use of white light makes it possible to connect fringe orders across a step even if the step height is greater than λ/4.

An excellent way of obtaining good height measurements with large steps or rough surfaces is to use a white light source and the coherence peak sensing approach described below.

In the vertical scanning coherence peak sensing mode of operation a broad spectral width light source is used. Due to the large spectral bandwidth of the source, the coherence length of the source is short, and good contrast fringes will be obtained only when the two paths of the interferometer are closely matched in length as shown in Figure 5. Thus, if in the interference microscope the path length of the sample arm of the interferometer is varied, the height variations across the sample can be determined by looking at the sample position for which the fringe contrast is a maximum. In this measurement there are no height ambiguities and since in a properly adjusted interferometer the sample is in focus when the maximum fringe contrast is obtained, there are no focus errors in the measurement of surface microstructure (12-16).

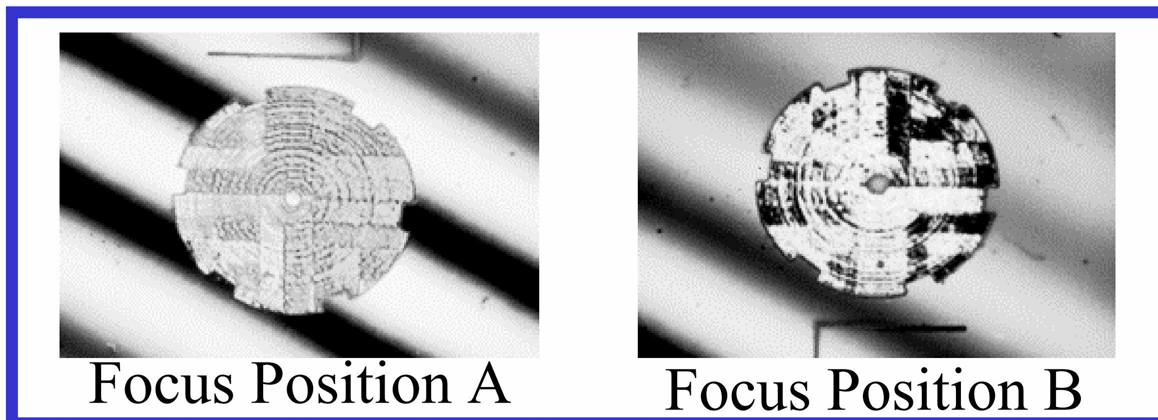

Figure 5. Good contrast fringes are obtained only when the interferometer paths are matched. (Sample is a micro-machined piece of silicon.)

The major drawback of this type of scanning interferometer measurement is that only a single surface height is being measured at a time and a large number of measurements and calculations are required to determine a large range of surface height values. One method for processing the data that gives both fast and accurate measurement results is to use conventional communication theory and fast computers with efficient software to demodulate the envelope of the fringe signal to determine the peak of the fringe contrast.

Figure 6 shows the irradiance at a single sample point as the sample is translated through focus. It should be noted that this signal looks a lot like an amplitude modulated (AM) communication signal. To obtain the location of the peak, and hence the surface height information, this irradiance signal is detected using a CCD array. The signal is sampled at fixed intervals, such as every 80 or 240 nm, as the sample path is varied. Low frequency and DC signal components are removed from the signal by digital high pass filtering. The signal is next rectified by square-law detection and digitally low pass filtered. The peak of the low pass filter output is located and the vertical position corresponding to the peak is noted. Interpolation between sample points can be used to increase the resolution of the instrument beyond the sampling interval. This type of measurement system produces fast, non-contact, true three-dimensional area measurements for both large steps and rough surfaces to nanometer precision.

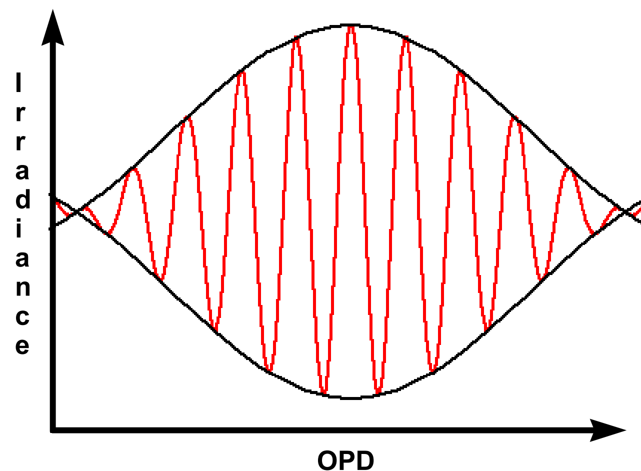

Figure 6. Irradiance at a single sample point as the sample is translated through focus.

Figure 7 shows a simplified schematic of a coherence peak sensing interference microscope. The configuration shown in Figure 7 utilizes a two-beam Mirau interferometer at the microscope objective. Typically the Mirau interferometer is used for magnifications between 10 and 50X, a Michelson interferometer is used for low magnifications, and the Linnik interferometer is used for high magnifications. A separate magnification selector is placed between the microscope objective and the CCD camera to provide additional image magnifications. A tungsten halogen lamp is used as the light source. Light reflected from the test surface interferes with light reflected from the reference. The resulting interference pattern is imaged onto the CCD array. Also, output from the CCD array is digitized and read by the computer. The Mirau interferometer is mounted on either a piezoelectric transducer (PZT) or a motorized stage so that it can be moved. During this movement, the distance from the lens to the reference surface remains fixed. Thus, a phase shift is introduced into one arm of the interferometer. By introducing a phase shift into only one arm while recording the interference pattern that is produced, it is possible to perform either phase-shifting interferometry or vertical scanning coherence peak sensing interferometry.

Figure 8 shows typical results obtained measuring a micro-machined piece of silicon.

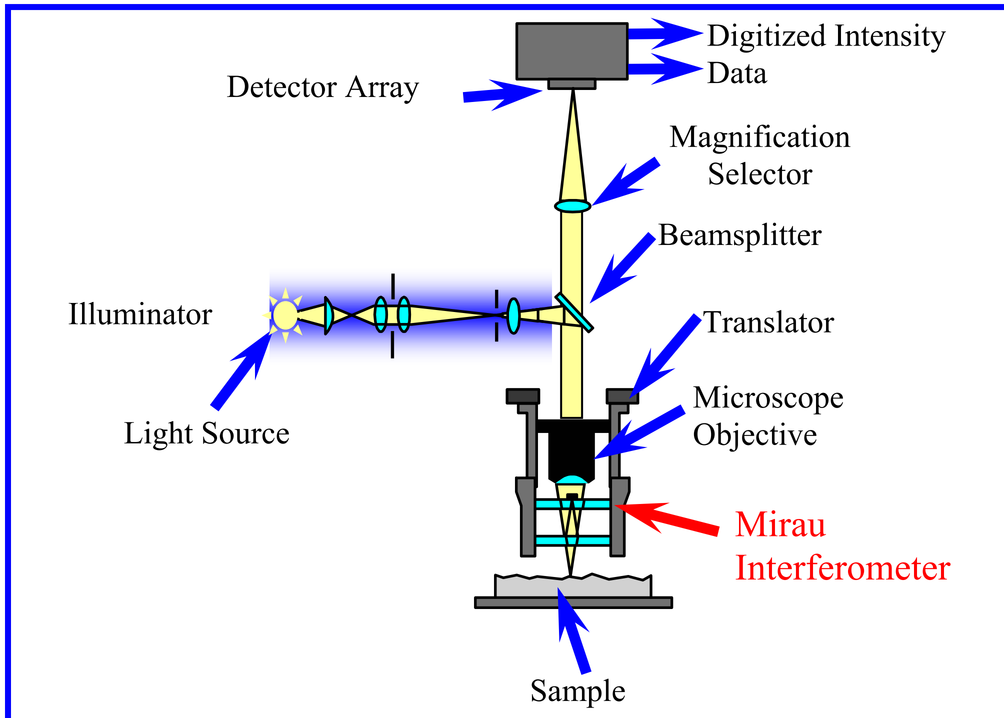

Figure 7. Optical schematic of interference microscope used for measurement of fine surface structure.

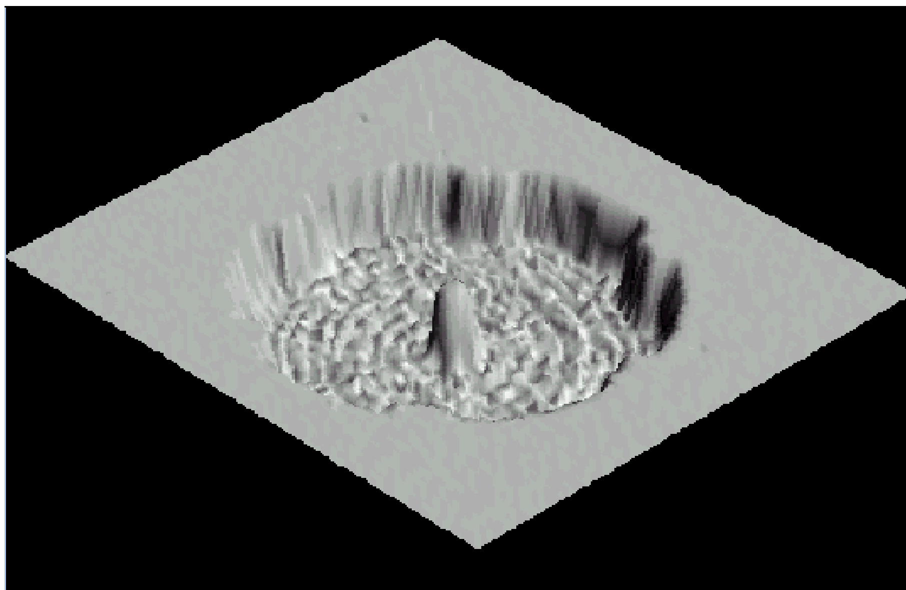

Figure 8. Results obtained using a vertical scanning coherence peak sensing measurement of a micro-machined silicon part. For this example the RMS of the surface is 2.3 microns and the P-V is 6.16 microns.

4. WHITE LIGHT SCATTERPLATE INTERFEROMETER

The scatterplate interferometer invented by Jim Burch in 1953 is one of the cleverest devices ever invented (17-18). The scatterplate interferometer is a common path interferometer that automatically matches interferometer paths so a zero order fringe is obtained whose position is independent of wavelength. The configuration of a scatterplate interferometer for testing spherical mirrors is shown in Figure 9. A magnified image of the scatterplate is shown in the upper left corner of the figure. A small circular aperture is illuminated with a laser or broadband source producing a source of limited extent for the interferometer. A focusing lens is used to image the source onto the test mirror by way of a beam splitter that removes the source from the path of the return beam and a scatterplate. The scatterplate is placed at the center of curvature of the test mirror. Part of the light incident on the scatterplate scatters illuminating the entire mirror surface and part of it passes directly through imaging to a point on the test mirror. After reflecting off the test surface the light again propagates through the scatterplate scattering a portion of the beam. Finally, a focusing lens is used to image the interference fringes onto a screen or detector.

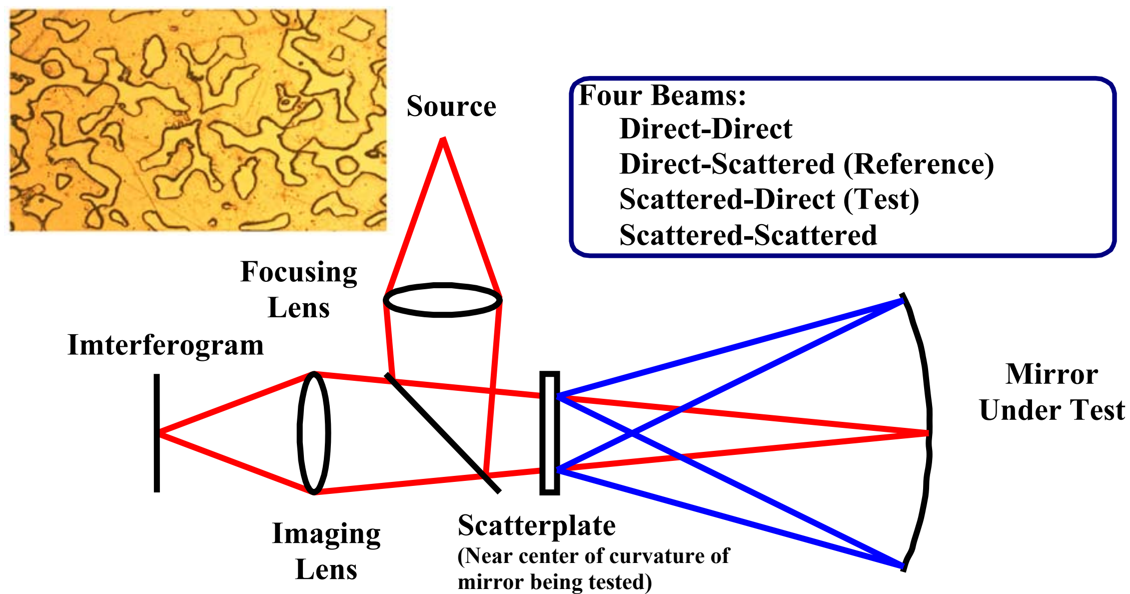

Figure 9. Scatterplate Interferometer for Testing Concave Mirrors.

To understand what produces the interference fringes we need to look more closely at the effect of the scatterplate. Each time the light encounters the scatterplate some of it is scattered and a portion passes directly through the plate. Since the scatterplate is traversed twice there are four permutations of the beam that arrive in the image plane: 1) Scattered-Scattered, 2) Scattered-Direct, 3) Direct-Scattered, and 4) Direct-Direct. An examination of each of these combinations will uncover their role in producing fringes. The direct-direct beam passes directly through the scatterplate both times it is encountered forming an image of the source called the “hot spot” in the image plane. Since the “hot spot” is never scattered, it does not contribute to the production of interference fringes. Similarly, the scattered-scattered beam does not play a role in the formation of interference fringes. The light is scattered both times it passes through the scatterplate producing background irradiance in the image plane. The direct-scattered beam is the reference beam of the interferometer. The light passes directly through the scatterplate on the first pass and forms an image of the source on the test surface. If the image of the source is small enough the phase variations introduced into the beam on reflection are negligible. On the return leg the light is scattered. The scattered-direct beam serves as the test beam of the interferometer. The light is scattered on its initial pass through the scatterplate illuminating the entire test mirror. Any departures from a sphere will introduce phase variations in the beam. The light then passes directly through the scatterplate producing fringes when it interferes with the reference beam.

It seems unlikely that two beams of light that have been scattered at different positions in the interferometer could possibly produce interference fringes. In general, the process described above would not produce meaningful interference fringes, however if the scatterplate has inversion symmetry (18) interference fringes showing the quality of the mirror under test are obtained. Inversion symmetry means that each scatter point has an exact twin located directly opposite the center point of the scatterplate as shown in Figure 10. The reason inversion symmetry works is revealed by examining individual scatter points and their effect on the reference and test beams. Keep in mind that examining individual points is not the complete story. Summing the wavefronts from all of the scatter points forms the contour fringes. Figure 10a summarizes the effect of inversion symmetry for a perfectly aligned system. When the incident light interacts with the scatterplate, the light scattered at scatter point S(x,y) acts like a point source. Since the scatterplate is located at the center of curvature of the test mirror, point S(x,y) is imaged back into the plane of the scatterplate at the conjugate point S'(x,y). The reference beam passes directly through the scatterplate reflects off the test mirror and scatters at point S(-x,-y). With inversion symmetry and proper alignment point S(x,y) and S(-x,-y) are scattered in exactly the same manner and the test and reference beams both appear as point sources located at point S(-x,-y). As a result, the phase change due to scattering is the same for both beams.

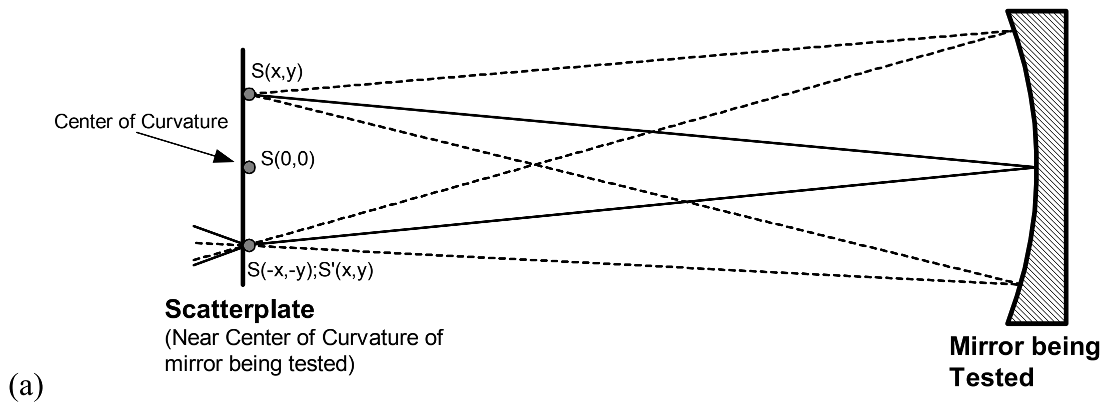

(a)

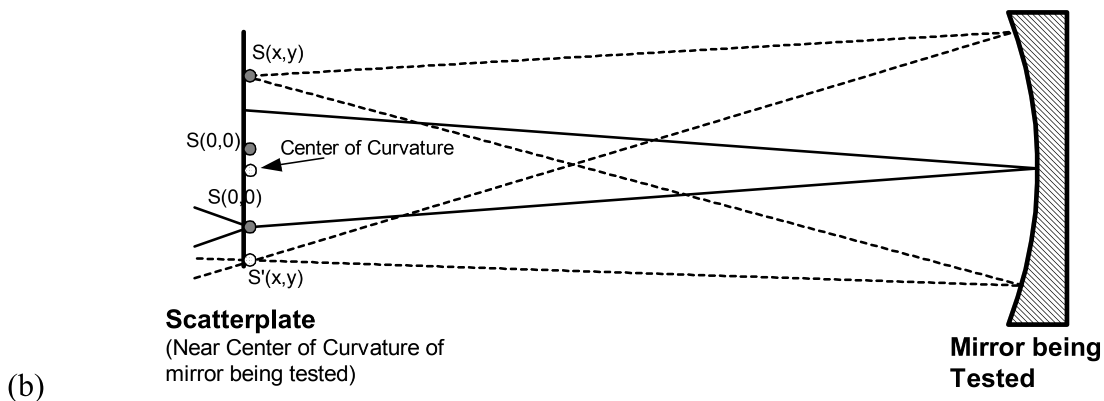

(b)

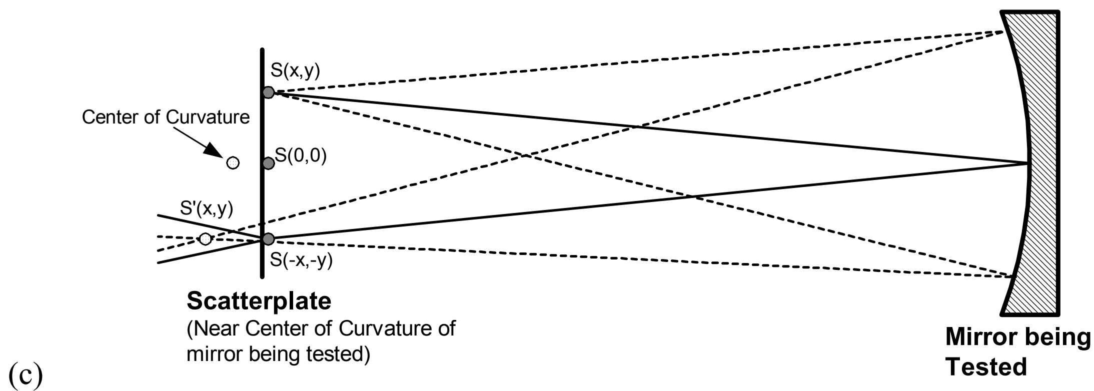

Figure10. Point-To-Point Analysis of Inversion Symmetry: (a) Perfect Alignment, (b) Lateral misalignment of Scatterplate, (c) Longitudinal Misalignment of Scatterplate.

The above discussion of inversion symmetry was for a system with perfect alignment. The effect of misalignment of the scatterplate will now be discussed. Lateral movement of the scatterplate produces tilt in the contour fringes. Figure 10b demonstrates the consequence of not aligning the center point of the scatterplate with the axis of the interferometer. The image of S(x,y), although still in the plane of the scatterplate, no longer coincides with the symmetric point S(-x,-y). The result is tilt in the contour fringes produced by the interference of two laterally shifted point sources. Similarly, longitudinal misalignment of the scatterplate adds defocus to the contour fringe pattern. Figure 10c shows the effect of not placing the scatterplate at the center of curvature of the test mirror. The image of point S(x,y) is still at the same lateral position as the symmetric point S(-x,-y), however it no longer lies in the plane of the scatterplate. The interference of the two longitudinally shifted point sources produces defocus in the contour fringes. Adjusting the scatterplate position adds an important flexibility for minimizing the number of contour fringes across the image plane.

A typical interferogram is shown in Figure 11. The source in this case consisted of several laser lines. It should be noted that the zero order fringe passes through the hot spot. For this fringe the two interferometer paths are matched.

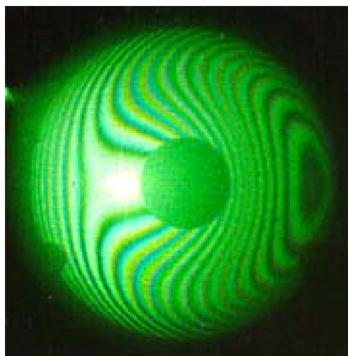

Figure 11. Typical scatterplate interferogram.

Recently several papers have been published showing techniques for phase-shifting scatterplate interferometers (19-21).

5. CONCLUSIONS

Three typical white light interferometers have been presented in this paper. The first interferometer, the grating interferometer, not only works with white light sources, but it is truly achromatic for a spherical wavefront illuminating the grating. Since interferometer path lengths must be nearly matched in a white light interferometer, spurious interference fringes are not a problem. Also, knowing that the paths are matched when the zero order fringe is obtained gives us a very powerful measurement tool as illustrated in the second interferometer, the vertical scanning or coherence probe interferometer. The last interferometer, the scatterplate interferometer, is very neat in that the zero order fringe is automatically obtained when fringes are obtained. While white interferometry is certainly not new, amazing things can be performed by combining rather old white light interferometry techniques with modern electronics, computers, and software. It is also neat to remember that beautiful interferograms are also obtained using a white light interferometer.

6. REFERENCES

1. Yu. N. Denisyuk, “Photographic reconstruction of the optical properties of an object in its own scattered radiation field,” *Sov. Phys.-Dokl*. **7**, p. 543, 1962.
2. Yu. N. Denisyuk, “On the reproduction of the optical properties of an object by the wave field of its scattered radiation,” Pt. I, *Opt. Spectrosc*. (USSR) **15**, p. 279, 1963.
3. Yu. N. Denisyuk, “On the reproduction of the optical properties of an object by the wave field of its scattered radiation,” Pt. II, *Opt. Spectrosc*. (USSR) **18**, p. 152, 1965.
4. Byung Jin Chang, Rod C. Alferness, Emmett N. Leith, “Space-invariant achromatic grating interferometers: theory (TE),” *Appl. Opt*., **14**, p. 1592, 1975.
5. Emmett N. Leith and Gary J. Swanson, “Achromatic interferometers for white light optical processing and holography,” *Appl. Opt*., **19**, p. 638, 1980.
6. Yih-Shyang Cheng, Emmett N. Leith, “Successive Fourier transformation with an achromatic interferometer,” *Appl. Opt*., **23**, p. 4029, 1984.
7. Emmett N. Leith, Robert R. Hershey, “Transfer functions and spatial filtering in grating interferometers,” *Appl. Opt*. **24**, p. 237, 1985.
8. J. C. Wyant, “White Light Extended Source Shearing Interferometer,” *Appl. Opt*., **13**, pp. 200-203, 1974.
9. Yeou-Yen Cheng and J. C. Wyant, "Two-wavelength phase shifting interferometry," Appl. Opt. 23(24), pp. 4539-4543, 1984.
10. Yeou-Yen Cheng and James C. Wyant, "Multiple-wavelength phase-shifting interferometry," Appl. Opt. 24(6). Pp. 804-807, 1985.
11. K. Creath, Y.-Y. Cheng, and J. C. Wyant, "Contouring aspheric surfaces using two-wavelength phase-shifting interferometry," Optica Acta 32(12), pp. 1455-1464, 1985.
12. M. Davidson, K. Kaufman, I. Mazor, and F. Cohen, "An Application of Interference Microscopy to Integrated Circuit Inspection and Metrology," Proc. SPIE, 775, 233-247, 1987.
13. G. S. Kino and S. Chim, "Mirau Correlation Microscope," Appl. Opt. 29, pp. 3775-3783, 1990.
14. T. Dresel, G. Hausler, and H. Venzke, "Three-dimensional sensing of rough surfaces by coherence radar," Appl. Opt. 31(7):919-3925, 1992.
15. P. J. Caber, "An Interferometric Profiler for Rough Surfaces," Appl. Opt. 32 (19), pp. 3438-3441, 1993.
16. James C. Wyant, "Computerized interferometric measurement of surface microstructure," Proc. SPIE 2576, pp.122-130, 1995.
17. J. M. Burch, “Scatter Fringes of Equal Thickness,” Nature 171, p. 889, 1953.
18. J. M. Burch, “Interferometry in Scattered Light,” *Optical Instruments and Technique*s, J.H. Dickson, ED.,Oriel Press, England, pp. 220-229, 1970.
19. Huang, Junejei et. al., “Fringe Scanning Scatter Plate Interferometer using a Polarized Light”, *Opt. Com*m., **68**, pp. 235-238, 1988.
20. Su, Der-Chin and Lih Horng Shyu, “Phase-shifting Scatter Plate Interferometer Using a Polarization Technique,” *J. Mod. Opt*., **38**, pp. 951-959, 1991.
21. Michael B. North-Morris, Jay VanDelden, and James C. Wyant, “Phase-shifting birefringent scatterplate interferometer,” Appl. Opt. **41**, pp. 668-677, 2002.